*Inorg. Chem.* **2007**, *46*, 2682–2690


# Effect of the Metal Environment on the Ferromagnetic Interaction in the Co–NC–W Pairs of Octacyanotungstate(V)–Cobalt(II) Three-Dimensional Networks

**Sergiu Clima,[†] Marc F. A. Hendrickx,[†] Liviu F. Chibotaru,*[,†] Alessandro Soncini,[†] Vladimir Mironov,[‡] and Arnout Ceulemans[†]**

*Laboratorium voor Kwantumchemie, Katholieke Universiteit Leuven, Celestijnenlaan 200F, B-3001 Leuven, Belgium, and Russian Academy of Sciences, AV Shubnikov Institute of Crystallography, Leninskii Pr 59, Moscow 117333, Russia*

Received December 8, 2006

State of the art CASSCF and CASPT2 calculations have been performed to elucidate the nature of ferromagnetism of $Co^{II}$–NC–$W^{V}$ pairs in the three-dimensional compound $[\{W^{V}(CN)_2\}_2\{(\mu\text{-}CN)_4Co^{II}(H_2O)_2\}_3\cdot 4H_2O]_n$, which has been recently synthesized and investigated by a number of experimental techniques (Herrera, J. M.; Bleuzen, A.; Dromzée, Y.; Julve, M.; Lloret, F.; Verdaguer, M. *Inorg. Chem.* **2003**, *42*, 7052–7059). In this network, the Co ions are in the high-spin ($S = {}^3/_2$) state, while the single unpaired electron on the W centers occupies the lowest orbital of the $d_{z^2}$ type of the 5d shell. In agreement with the suggestion made by Herrera et al., we find that the ferromagnetism is due to a certain occupation scheme of the orbitals from the parent octahedral $t_{2g}$ shell on $Co^{II}$ sites, in which the orbital accommodating the unpaired electron is orthogonal to the $d_{z^2}$ orbitals of the surrounding W ions. We investigate the stabilization of such an orbital configuration on the Co sites and find that it cannot be achieved in the ground state of isolated mononuclear fragments $[Co^{II}(NC)_4(OH_2)_2]^{2-}$ for any conformations of the coordinated water molecules and Co–N–C bond angles. On the other hand, it is stabilized by the interaction of the complex with neighboring W ions, which are simulated here by effective potentials. The calculated exchange coupling constants for the $Co^{II}$–NC–$W^{V}$ binuclear fragments are in reasonable agreement with the measured Curie–Weiss constant for this compound. As additional evidence for the inferred electronic configuration on the Co sites, the ligand-field transitions, the temperature-dependent magnetic susceptibility, and the field-dependent low-temperature magnetization, simulated ab initio for the mononuclear Co fragments, are in agreement with the available data for another compound $[W^{IV}\{(\mu\text{-}CN)_4\text{-}Co^{II}(H_2O)_2\}_2\cdot 4H_2O]_n$ containing diamagnetic W and high-spin Co ions in an isostructural environment.

## Introduction

The growth of interest in the synthesis and characterization of molecular magnets started more than 2 decades ago.[1−4] To date, a large variety of polynuclear transition-metal complexes have been synthesized, with metal ions combined by a number of bridging ligands: oxo, oxalato, cyano, etc. The magnetic properties of polynuclear complexes and networks are known to be highly sensitive to geometry, especially to the bending angle of the bridging ligand.[2] In this respect, cyano-bridged compounds seem to be promising because their structural and magnetic properties can easily be tuned by combining $[M(CN)_n]^{m-}$ mononuclear-complex building blocks. As a result, a large number of cyano-bridged compounds of different dimensionality ranging from clusters to three-dimensional networks have been synthesized.[5−10] Cya-

* To whom correspondence should be addressed. E-mail: liviu.chibotaru@chem.kuleuven.be. Phone: (int.-32)16327424. Fax: (int.-32)16327992.
[†] Katholieke Universiteit Leuven.
[‡] AV Shubnikov Institute of Crystallography.

(1) Herrera, J. M.; Bleuzen, A.; Dromzée, Y.; Julve, M.; Lloret, F.; Verdaguer, M. *Inorg. Chem.* **2003**, *42*, 7052−7059.
(2) Kahn, O. *Molecular Magnetism*; VCH Publishers: New York, 1993.
(3) *Magnetism: Molecules to Materials*; Miller, J. S., Drillon, M., Eds.; Springer-Verlag: Berlin, Vols. I−V.
(4) *Magnetic Molecular Materials*; Gatteschi, D., Kahn, O., Miller, J. S., Palacio, F., Eds.; Kluwer: Dordrecht, The Netherlands, 1991.
(5) Mallah, T.; Thiebaut, S.; Verdaguer, M.; Veillet, P. *Science* **1993**, *262*, 1554.
(6) William, R. E.; Girolami, G. S. *Inorg. Chem.* **1994**, *33*, 5165.



10.1021/ic062345+ CCC: $37.00 
Published on Web 03/10/2007

nide bridges are also known to be good mediators of exchange interaction. This is mainly due to their preferential linear and strongly covalent binding to the transition metals, which leads to high values of antiferromagnetic exchange coupling constants, especially when metals from the second and third transition row are involved.[11] Strong antiferromagnetic interactions are the reason for the room-temperature ferrimagnetism, observed in some compounds of the Prussian blue family.[5,8] Given the local cubic symmetry on metal sites, the ferromagnetic interaction in Prussian blues is often achieved because it is merely determined by the orthogonality of magnetic orbitals on neighboring metal ions. Such an orthogonality can be easily controlled by a proper choice of transition-metal ions in this material.[5] However, in other cyano-bridged compounds, with lower symmetry of sites, the origin of ferromagnetism is not as evident as it is in Prussian blue based materials and requires additional investigations for its understanding.

Recently, Herrera et al.[1] have synthesized and characterized a new three-dimensional octacyanotungstate(V)−cobalt(II) compound, $[\{W^{V}(CN)_2\}_2\{(\mu\text{-}CN)_4Co^{II}(H_2O)_2\}_3\cdot 4H_2O]_n$ (**2**), with ferromagnetic coupling between neighboring Co and W ions. The authors of ref 1 also synthesized and investigated another compound, $[W^{IV}\{(\mu\text{-}CN)_4\text{-}Co^{II}(H_2O)_2\}_2\cdot 4H_2O]_n$ (**1**), with diamagnetic W ions and an isostructural environment of the Co ions. This allowed them to investigate thoroughly the electronic structure and magnetic properties of the common Co fragment $[Co^{II}(NC)_4(OH_2)_2]^{2-}$ by analyzing the difference absorption spectrum and difference susceptibility of the two compounds.

In this Article, we report the results of CASSCF/CASPT2 calculations of mononuclear $Co^{II}$ and binuclear $Co^{II}-NC-W^{V}$ fragments of the above compounds. We investigate the factors influencing the order of lowest electronic levels on the Co site and the origin of ferromagnetic interaction in Co−W pairs. We find, in particular, the major role played by other W ions surrounding the Co ion of a given Co−NC−W pair in the observed ferromagnetic coupling. In addition, we calculate the ligand-field spectra, the magnetization, and the magnetic susceptibility of an isolated $Co^{II}$ fragment and compare the results with experimental data in ref 1.

## Computational Details

The crystal structure of $[Co(NC)_4(OH_2)_2]^{2-}$ fragments in compounds **1** and **2** shows Co−NC bonds deviating from linearity by 13−17° (except for two Co−NC bonds in **1**, which are bent by 24°). At the same time, the positions of the N atoms exhibit a small deviation from $C_4$ symmetry,[1] so that the structure of the fragments is close to $C_{2h}$ symmetry. In all calculations presented here, we adopted this idealized geometry of the Co fragments (Figure 1).

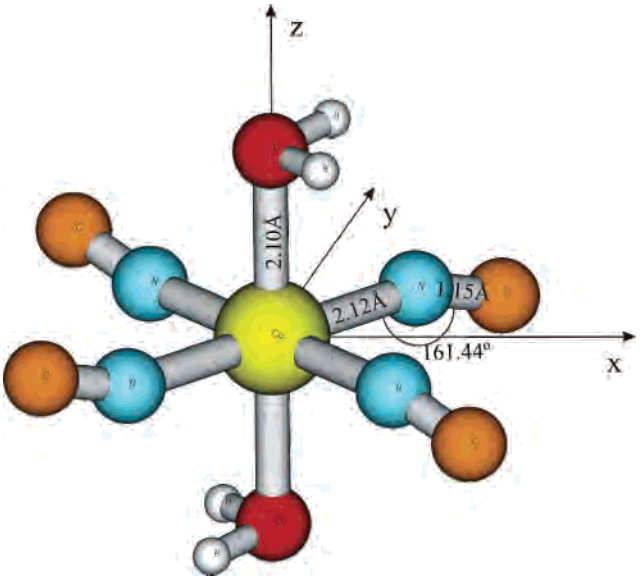


**Figure 1.** Geometrical parameters of the $[Co(NC)_4(OH_2)_2]^{2-}$ fragment in $C_{2h}$ symmetry, as used in calculations and the coordinate system.

The origin of the coordinate system was chosen on the Co atom with the axis *y* directed along the twofold rotational axis and *xz* being the mirror plane (the O atoms are situated on the *z* axis, and the N atoms are positioned between the *x* and *y* axes). In all calculations, averaged experimental bond distances were used: 2.12 Å for Co−N, 1.15 Å for C−N, and 2.10 Å for Co−O.

The calculations have been done by the CASSCF/CASPT2 method using the quantum chemistry package *MOLCAS 6.0*.[12] C, N, O, and H atoms were described by ANO-RCC-VDZP quality basis sets, whereas for the Co atom, seven s-type, six p-type, five d-type, and two f-type orbitals of the same ANO-RCC basis set (as available in the *MOLCAS* chemical software package) were chosen.[12] After calculation of the CASSCF wave functions, they were used in the CASPT2 treatment of the dynamic electron correlations. All but the core electrons of C, O, N (1s) and Co (1s, 2s, 2p, 3s) were correlated at the CASPT2 level. Because the crystallographic data do not provide the position probability of the H atoms, a manual geometry optimization of the H atoms was done at the CASPT2 level, employing an active space that includes the five 3d orbitals and the five 4d orbitals to account for the double-shell effect. The optimization was carried out by imposing $C_{2h}$ symmetry and started from the bond distances and angles of the free water molecule by optimizing the O−H bond distance. With the obtained O−H distance, the H−O−H angle was optimized in a second step. The geometry optimization was finalized by an energy minimization of the angle between the plane of the water molecules and the plane of the four N atoms. The following geometric parameters for the water molecules were obtained: an O−H bond distance of 0.974 Å and an H−O−H angle of 104.72°. The HOH plane is 8° bent relative to the plane of the four N atoms. A subsequent optimization of the O−H distances by freezing the angles to these values gave no significant changes. In addition, several structures differing in the orientation of molecular water plane (vs the $N_4$ plane) and Co−N−C bond angles were investigated in order to reveal their influence on the excitation energies. All of these conformations are depicted in Figure 2. Conformations **I** and **III** possess experimental Co−N−C bond angles (161.44°), while

(7) El Fallah, S. M.; Rentschler, E.; Caneschi, A.; Sessoli, R.; Gatteschi, D. *Angew. Chem.* **1996**, *108*, 2081.
(8) Ferlay, S.; Mallah, T.; Ouahes, R.; Veillet, P.; Verdaguer, M. *Nature* **1995**, *378*, 701.
(9) Kahn, O.; Larionova, J.; Quahab, L. *Chem. Commun.* **1999**, 945.
(10) Larionova, J.; Willemin, S.; Donnadieu, B.; Henner, B.; Guérin, C.; Gillon, B.; Goujon, A. *J. Phys. Chem. Solids* **2004**, *65*, 677.
(11) Ruiz, E.; Rodríguez-Fortea, A.; Alvarez, S.; Verdaguer, M. *Chem.—Eur. J.* **2005**, *11*, 2135.
(12) Karlström, G.; Lindh, R.; Malmqvist, P.-Å.; Roos, B. O.; Ryde, U.; Veryazov, V.; Widmark, P.-O.; Cossi, M.; Schimmelpfennig, B.; Neogrady, P.; Seijo, L. *Comput. Mater. Sci.* **2003**, *28*, 222.

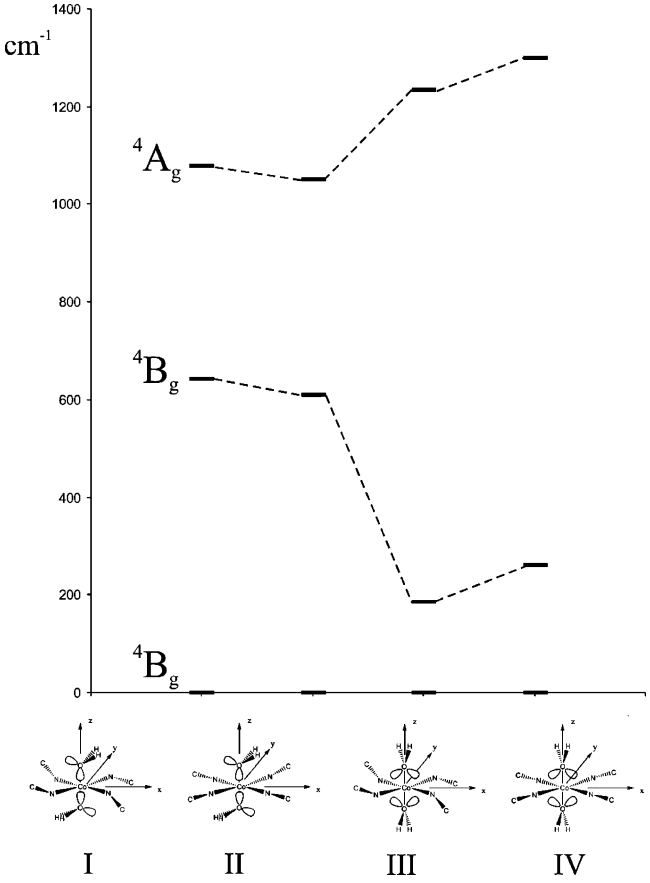


**Figure 2.** Splitting pattern of the $^4T_{1g}$ components in different calculated conformations of the water ligands and Co−C−N bond angles.

the other two conformations have straight Co−N−C bonds. The plane of the water ligands either is perpendicular to the plane of the four N atoms (**III** and **IV**) or was set at the CASPT2-optimized value for this angle of 8° (**I** and **II**). The influence of the four neighboring octacyanotungsten sites on the $[Co(NC)_4(OH_2)_2]^{2-}$ wave function has been simulated by employing available ($Cs^+$ and $Ba^{2+}$) ab initio model potentials (AIMPs) that closely resemble in nature the $W^V$ centers, as well as point charges (PCs) at the experimental positions of the respective centers. The magnetic properties of the mononuclear $Co^{II}$ fragment have been investigated by applying a newly developed ab initio methodology,[13] based on the CASSCF/RASSI wave functions and CASPT2 energies with spin−orbit interaction included.

In order to estimate the magnetic interaction parameters of the binuclear fragment, several geometrical conformations of $[(H_2O)_2(CN)_3Co^{II}(NC)W^V(CN)_7]^{4-}$ have been treated at the CASPT2 level, employing effective core potential basis sets for Co and W and ANO-S for C, N, and O. In order to simplify the calculations, a $C_s$-symmetrized conformation of the binuclear fragment has been used. In several sets of computations, we simulated the rest of the crystal by using different AIMPs and PCs at the other three $W^V$ sites. The desired AIMPs are not available for cyanide groups and W ions; hence, we had to restrict ourselves to the description of the W ions bridged to $Co^{2+}$ through the cyanide ligands with AIMPs close by nature to a $W^V$ center.[18] We performed several CASSCF/CASPT2 calculations for the binuclear complex that included simple PCs of +1.5 or AIMPs ($Cs^+$or $Ba^{2+}$) at the three remaining $W^V$ positions around the $[(H_2O)_2(CN)_3Co^{II}(NC)W^V(CN)_7]^{4-}$ entity.

## Results and Discussion

**Ligand-Field Spectrum of an Isolated $Co^{II}$ Fragment.** For the octahedral $^4T_{1g}$ high-spin ground state of a $t_{2g}^5e_g^2$ configuration, taking into account the axial distortion, Herrera et al.[1] proposed a 100 $cm^{-1}$ energy gap of unknown sign between the $^4A_2$ and $^4E$ states of the $C_{4v}$ $Co^{II}$ center. Because our calculated conformations include the positions of the H atoms and because in some conformers the cyanide bridging ligands are bent as in the experimental structure, the symmetry is lowered to a minimal $C_{2h}$ so that the $^4E$ state is further split into two $^4A_g$ and $^4B_g$ states. Table 1 presents the CASPT2 energies of all ligand-field states relevant to the electronic spectrum, and Figure 2 shows the CASPT2 $C_{2h}$ splitting of the octahedral high-spin ground state. According to this splitting, our CASPT2 calculations give for all four conformers of $[Co(NC)_4(OH_2)_2]^{2-}$ a $^4B_g$ ground state, in which the two $d_\sigma$ orbitals, $d_{z^2}$ and $d_{xy}$, and one $d_\pi$ orbital, $d_{x^2-y^2}$, are singly occupied, while the other two $d_\pi$ orbitals, $d_{xz}$ and $d_{yz}$, are doubly occupied. One can see from Figure 2 that the effect of the orientation of the water ligands on the relative energies of the components of the quartet $^4T_{1g}$ is much more pronounced than the straightening of the Co−N−C angles. The variation of the splittings from conformer **I** (completely optimized HOH and experimental Co−N−C bond angle) to conformer **II** (HOH unchanged and linear Co−N−C) is much smaller in comparison with the case when the Co−N−C angles are kept bent in their experimental positions and the HOH planes change their positions relative to the $N_4$ plane (**I** → **III**). Comparing total CASPT2 energies for various conformers, we may conclude that the perpendicular position of the water molecules has a much more pronounced destabilizing effect than the straightening of the Co−NC bonds. We also studied other conformations, with different relative orientations of the two water ligands with respect to each other and to the bridging cyanides. Among all of them, conformer **I** was always found to be the lowest in energy. We use it, therefore, in further discussion of the ligand-field spectrum of the $[Co(NC)_4(OH_2)_2]^{2-}$ fragment. It should be noted that, in all studied conformers, the order of the three $^4T_{1g}$ components remains unchanged. As will be seen further, the sign of the exchange interaction within nearest-neighboring $Co^{II}-W^V$ pairs is

(13) Chibotaru, L. F.; et al., unpublished. The CASSCF wave functions of several lowest excited states including spin−orbit coupling effects after CASPT2 treatment are used to calculate the magnetic dipole matrix elements, with which the *g* tensor, the magnetic susceptibility, and the magnetization are evaluated.

(14) Anderson, P. W. *Phys. Rev.* **1959**, *115*, 2.

(15) Chibotaru, L. F.; Mironov, V. S.; Ceulemans, A. *Angew. Chem., Int. Ed.* **2001**, *40*, 4429.

(16) The nearest neighbors of the Co fragment are four W atoms, which bind to it via the cyanide groups surrounding the Co ion (Figure 3). Because $W^V$ ions contain one unpaired electron each, their orbitals, according to the methodology of the CASSCF approach, should be included in the active space. This exceeds, however, the possibilities of the current version of *MOLCAS*.

(17) Seijo, L.; Barandiarán, Z. In *Computational Chemistry: Reviews of Current Trends*; Leszczyński, J., Ed.; World Scientific: Singapore, 1999; Vol. 4, p 55.

(18) The actual charge of the W ion in the octacyanide environment does not correspond, of course, to its formal valence (V), being considerably smaller. It should be reduced even further if one wishes to simulate the electrostatic effect of the surrounding negatively charged cyanide groups.

**Table 1.** CASPT2 Terms of the Fragment $[Co(NC)_4(OH_2)_2]^{2-}$ of Compound **1**

| | | CASPT2 | | | | |
|---|---|---|---|---|---|---|
| $Co^{II}$ $O_h$ | state* $C_{2h}$ | I | II | III | IV | expt ($cm^{-1}$) |
| $^4T_{1g}$ $t_{2g}^5e_g^2$ | $^4B_g^1$ $(xz)^2(yz)^2(x^2-y^2)^1(z^2)^1(xy)^1$ | 0 | 0 | 0 | 0 | |
| | $^4B_g^2$ $(xz) \rightarrow (x^2-y^2)$ | 643 | 609 | 185 | 261 | |
| | $^4A_g^1$ $(yz) \rightarrow (x^2-y^2)$ | 1 078 | 1 050 | 1 234 | 1 300 | |
| $^4T_{2g}$ $t_{2g}^4e_g^3$ | $^4A_g^2$ $(xz, yz) \rightarrow (x^2-y^2, z^2)$ | 8 162 | 8 239 | 6 891 | 7 033 | |
| | $^4A_g^3$ $(xz) \rightarrow (xy)$ 70% $(yz) \rightarrow (z^2)$ 30% | 9 035 | 9 217 | 8 443 | 8 700 | **8784** |
| | $^4B_g^3$ $(xz) \rightarrow (z^2)$ 30% $(yz) \rightarrow (xy)$ 70% | 9 068 | 9 243 | 8 662 | 8 891 | |
| $^4A_{2g}$ $t_{2g}^3e_g^4$ | $^4B_g^4$ $(xz, yz) \rightarrow (z^2, xy)$ | 18 741 | 19 054 | 17 390 | 17 802 | **16 639** |
| $^4T_{1g}$ $t_{2g}^4e_g^3$ | $^4A_g^4$ $(xz) \rightarrow (xy)$ 30% $(yz) \rightarrow (z^2)$ 70% | 21 193 | 21 390 | 20 424 | 20 689 | |
| | $^4B_g^5$ $(xz) \rightarrow (z^2)$ 70% $(yz) \rightarrow (xy)$ 30% | 21 399 | 21 427 | 20 453 | 20 599 | **20 575** |
| | $^4B_g^6$ $(xz, yz) \rightarrow (xy, x^2-y^2)$ | 24 771 | 25 067 | 24 963 | 25 313 | |
| $^2E_g$ $t_{2g}^6e_g^1$ | $^2A_g^1$ $(xy) \rightarrow (x^2-y^2)$ | 10 104 | 9 900 | 10 063 | 9 946 | |
| | $^2B_g^1$ $(z^2) \rightarrow (x^2-y^2)$ | 12 760 | 12 700 | 14 098 | 14 153 | |
| $^2T_{1g}$ $t_{2g}^5e_g^2$ | $^2A_g^2$ | 18 048 | 17 985 | 17 042 | 17 028 | |
| | $^2B_g^2$ | 18 265 | 18 250 | 17 604 | 17 640 | |
| | $^2B_g^3$ | 18 382 | 18 348 | 18 376 | 18 450 | |
| $^2T_{2g}$ $t_{2g}^5e_g^2$ | $^2A_g^3$ | 19 643 | 19 623 | 20 030 | 20 127 | |
| | $^2A_g^4$ | 20 198 | 20 252 | 17 283 | 19 317 | |
| | $^2B_g^4$ | 19 168 | | 19 208 | 19 313 | |

essentially determined by the nature of the ground state. Because this remains the same for all calculated conformers, in particular, for arbitrary orientations of H atoms in the coordinated water molecules, the exact orientation of the water molecules is actually not important for further consideration. For the same reason, we did not consider the effect of hydrogen bonding on the orientation of the water molecules, although this may change the equilibrium conformation **I**.

The electronic spectrum of $[Co(NC)_4(OH_2)_2]^{2-}$, derived as the difference between the UV−vis spectra of **1** and of the precursor $K_4[W(CN)_8]\cdot 2H_2O$, exhibits two absorption bands at 8784 and 20 575 $cm^{-1}$ and a weak shoulder at 16 639 $cm^{-1}$.[1] We calculated the ligand-field states arising from the second $^4T_{2g}$ quartet of $Co^{II}$ to have one component situated around 8000 $cm^{-1}$ with respect to the ground state and the other two components lying around 9000 $cm^{-1}$. In the cases of conformations with water molecules perpendicular to the $N_4$ plane, the lowest component of $^4T_{2g}$ is around 1000 $cm^{-1}$ lower than that for the conformations with optimized positions of water ligands. The transitions to these $^4T_{2g}$ components are likely to be responsible for the first band of the difference spectrum at 8784 $cm^{-1}$. Some intensity is borrowed from spin-allowed transitions to the components of the doublet $^2E_g$ situated close in energy (10 000−14 000 $cm^{-1}$), but it is probably too small to be observed in the spectra. The excitation of one electron from the $d_\pi$ orbitals ($d_{x^2-y^2}$, $d_{xz}$, and $d_{yz}$) to the $d_\sigma$ orbitals ($e_g$: $d_{z^2}$ and $d_{xy}$) gives rise to a $^4T_{1g}$ state (Table 1). The rhombic distortion induced by water ligands and bent cyanides splits $^4T_{1g}$ into three quartets, with the highest one being situated around 25 000 $cm^{-1}$ and the other two lying around 21 000 $cm^{-1}$ (the conformation of water and cyanide ligands has a quite insignificant effect on the splitting of the $^4T_{1g}$ components). The excitations to these states are probably responsible for the second band in the spectrum at 20 575 $cm^{-1}$. The reported shoulder at 16 639 $cm^{-1}$ could be a transition to the $^4A_{2g}$ state, which is somewhat overestimated by our CASSCF/CASPT2 calculations and the models simulating the environment of the Co fragment discussed below. Also, it is not excluded that some intensity in the shoulder is due to the spin-forbidden transition to the components of the $^2T_{1g}$ state, for which we estimate a transition energy of around 18 000 $cm^{-1}$.

**Exchange Interaction in the $Co^{II}-W^V$ Binuclear Fragments.** The results of CASSCF/CASPT2 calculations for the lowest states of the $C_s$-symmetrized binuclear fragment $[(H_2O)_2(CN)_3Co^{II}(NC)W^V(CN)_7]^{4-}$ (Figure 3) are given in Table 2. With water ligands in the bent position (8°, not shown), we obtain an energy splitting between the lowest triplet and quintet states of 29 $cm^{-1}$, corresponding to an antiferromagnetic interaction in the Co−W dimer. The calculation in the same conformation of the binuclear complex but with the plane of water ligands perpendicular to the $N_4$ plane showed that the position of the water molecules has no impact on the triplet−quintet splitting ($\Delta E = 28$ $cm^{-1}$), with the triplet having the lowest energy. Also, test calculations with different Co−O bond lengths (1.9−2.1 Å) did not change the spin of the ground state, with the triplet−quintet gap being equal to 28 $cm^{-1}$. Calculations with the experimental $C_1$ geometry of the binuclear complex supported again an antiferromagnetic interaction between metal sites with almost the same energy gap, $\Delta E = 29$ $cm^{-1}$. Similar calculations for different positions of the water molecules did not modify again the spin of the ground state.

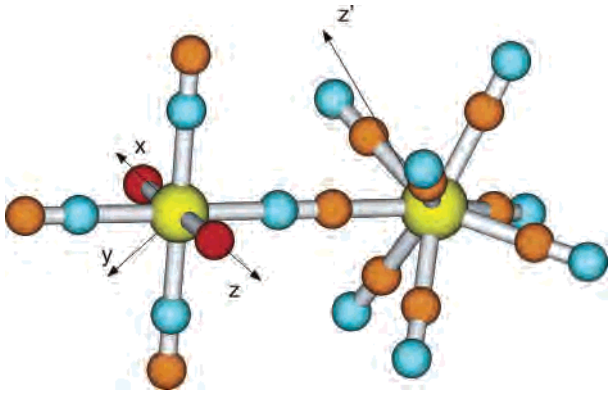


**Figure 3.** Co−W binuclear fragment in a $C_s$-symmetrized conformation (the coordinate system on the Co site is the same as that in Figure 1).

**Table 2.** CASSCF and CASPT2 Energies ($cm^{-1}$; Relativistic Effects Included) of the Lowest Triplets and Quintets and Their Natural Occupation Numbers (the $5d_{z'^2}$ on the $W^V$ Center Is Always Singly Occupied) in Different Embedding Schemes (ESs) and Active Spaces (ASs) of the Binuclear Co−W Fragment in $C_s$-Symmetrized Geometry

| | | | | 3d orbitals of Co[a] | | | | |
|---|---|---|---|---|---|---|---|---|
| AS/ES | state | CASSCF | CASPT2 | $x^2-y^2$ | $xy$ | $z^2$ | $xz$ | $yz$ |
| 8i6/− | $^3A'$ | 0 | 0 | 1.07 | 1.00 | 1.07 | 1.93 | 1.93 |
| 8i6/− | $^3A''$ | 294 | 236 | 1.91 | 1.00 | 1.09 | 1.09 | 1.91 |
| 8i6/− | $^5A'$ | 3 | 29 | 1.07 | 1.00 | 1.07 | 1.93 | 1.93 |
| 8i6/− | $^5A''$ | 289 | 230 | 1.91 | 1.00 | 1.09 | 1.09 | 1.91 |
| 8i6/PC(+1.5) | $^3A'$ | 107 | 181 | 1.09 | 1.08 | 1.00 | 1.92 | 1.92 |
| 8i6/PC(+1.5) | $^3A''$ | 5 | 20 | 1.92 | 1.00 | 1.08 | 1.92 | 1.08 |
| 8i6/PC(+1.5) | $^5A'$ | 116 | 230 | 1.08 | 1.08 | 1.00 | 1.92 | 1.92 |
| 8i6/PC(+1.5) | $^5A''$ | 0 | 0 | 1.92 | 1.00 | 1.08 | 1.92 | 1.08 |
| 8i6/AIMP($Cs^+$) | $^3A'$ | 0 | 0 | 1.07 | 1.07 | 1.00 | 1.93 | 1.93 |
| 8i6/AIMP($Cs^+$) | $^3A''$ | 243 | 178 | 1.91 | 1.09 | 1.00 | 1.09 | 1.91 |
| 8i6/AIMP($Cs^+$) | $^5A'$ | 5 | 18 | 1.07 | 1.07 | 1.00 | 1.93 | 1.93 |
| 8i6/AIMP($Cs^+$) | $^5A''$ | 238 | 155 | 1.91 | 1.09 | 1.00 | 1.09 | 1.91 |
| 8i6/AIMP($Ba^{2+}$) | $^3A'$ | -27 | 3 | 1.08 | 1.08 | 1.00 | 1.92 | 1.92 |
| 8i6/AIMP($Ba^{2+}$) | $^3A''$ | 5 | 13 | 1.92 | 1.00 | 1.08 | 1.92 | 1.08 |
| 8i6/AIMP($Ba^{2+}$) | $^5A'$ | -18 | 56 | 1.08 | 1.08 | 1.00 | 1.92 | 1.92 |
| 8i6/AIMP($Ba^{2+}$) | $^5A''$ | 0 | 0 | 1.92 | 1.00 | 1.08 | 1.92 | 1.08 |
| 14i9/PC(+1.5) | $^3A'$ | −777 | 230 | 1.07 | 1.06 | 1.00 | 1.94 | 1.94 |
| 14i9/PC(+1.5) | $^3A''$ | 5 | 11 | 1.93 | 1.00 | 1.07 | 1.93 | 1.07 |
| 14i9/PC(+1.5) | $^5A'$ | −767 | 285 | 1.06 | 1.06 | 1.00 | 1.94 | 1.94 |
| 14i9/PC(+1.5) | $^5A''$ | 0 | 0 | 1.93 | 1.00 | 1.07 | 1.93 | 1.07 |

[a] The active orbitals in the last two columns correspond to *xz* and *yz* only for A′ states but are combinations of these two for states of other symmetries.

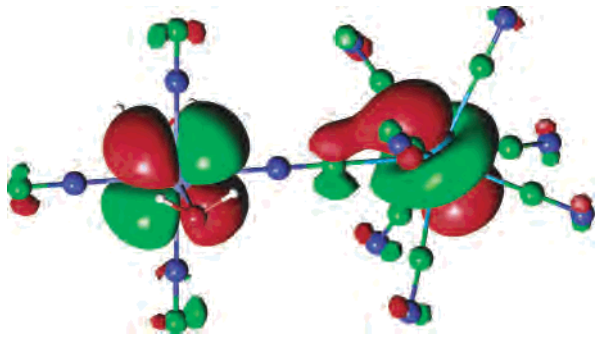

**Figure 4.** Antibonding active orbital of the $d_{xy}$(Co)−$d_{z'^2}$(W) type for the lowest triplet state of the binuclear fragment $[(H_2O)_2(CN)_3Co^{II}(NC)W^V(CN)_7]^{4-}$.

An inspection of the multielectron wave functions of the ground state has shown that in all studied geometrical conformations the main contribution comes from electronic configurations with singly occupied orbital $d_{x^2-y^2}$ on the $Co^{II}$ center. This orbital strongly mixes with the single magnetic orbital $d_{z'^2}$ on the $W^V$ site, which is seen from the shape of the corresponding active molecular orbital for the triplet wave function (Figure 4). As a result of this mixing, the unpaired spin in the $d_{x^2-y^2}$ orbital of Co can delocalize into the singly occupied $d_{z'^2}$ orbital of W and vice versa, leading to a strong antiferromagnetic kinetic contribution to the exchange interaction.[2,14] The other two orbitals from the octahedral $t_{2g}$ shell of Co, $d_{xz}$ and $d_{yz}$, do not mix with the $d_{z'^2}$ of W because of the mirror symmetry in the *xy* plane, which is imposed in the idealized geometry of the fragment (Figure 3). On the other hand, the two orbitals from the parent octahedral e shell of the Co site, $d_{z^2}$ and $d_{xy}$, can only mix with the $d_{z'^2}$ orbital of W via the $\sigma$ bonds of the bridging cyanide (again in the idealized geometry of the binuclear fragment). Such a mixing is expected, however, to be rather weak because in the square-antiprismatic geometry the CN groups point almost exactly to the node of the $d_{z'^2}$ orbital.[15] This can be inferred by inspecting the plots of the corresponding active orbitals for the triplet wave function of the binuclear fragment (Figure 1S in the Supporting Information).

The next step in our modeling was to take into account the crystal environment around the $Co^{II}$ center. It was not possible to include directly the closest atoms from the environment in the calculation because of intrinsic restrictions of the CASSCF method.[16] Therefore, we decided to model the environment by AIMPs.[17] The results are collected in Table 2. We can see that PCs of +1.5 and the $Ba^{2+}$ AIMPs bridged to the Co center lead to a ferromagnetic interaction with the quintet−triplet gaps of 3 and 20 $cm^{-1}$, respectively. The most reliable calculations performed were those with the extended active space that included three more occupied orbitals (14i9) and yielded an energy gap between the lowest quintet and triplet of $\Delta_{QT} = 11$ $cm^{-1}$. The inspection of the multielectron wave functions for the lowest states shows that in all of these calculations the main contribution comes from the configurations with a doubly occupied $d_{x^2-y^2}$ orbital on the $Co^{II}$ center. This means that the kinetic antiferromagnetic contribution to the exchange coupling is absent in these cases, which explains the obtained ferromagnetic coupling between Co and W sites. This conclusion supports the scenario of ferromagnetic coupling in compound **2** proposed by Herrera et al.[1]

Actually there are two nonequivalent Co sites in compound **2**, Co(1) and Co(2),[1] and the exchange-coupled fragments Co(1)−W and Co(2)−W are therefore nonequivalent as well. The main structural difference between them is the direction of the Co−NC bends, which are equally oriented in the case of Co(1) but have opposite orientations in the case of Co(2). Because we use in our calculations an idealized structural model (Figure 3), it equally applies to both types of binuclear fragments. Because all W ions are crystallographically equivalent, the orientation of the magnetic orbital $d_{z'^2}$ will be the same (translationally invariant) on all W sites. Despite different orientations of the axes of the Co−W pairs corresponding to four W ions surrounding a given Co site, the relative orientation of the four W magnetic orbitals $d_{z'^2}$ with respect to the Co orbitals will be similar; the same goes for the exchange interaction in the four fragments. This is clearly seen in Figure 2S in the Supporting Information, showing the arrangement of the W sites around a Co(2) fragment. The figure also shows the position of the $d_{z'^2}$ orbital in the idealized structure (Figure 3) relative to the actual position of the corresponding W ion in compound **2**. Although the resulting shift caused by the Co−NC bending is relatively large, the calculations of the exchange splitting in the idealized and experimental geometries of the fragment have shown practically no difference, as was mentioned above. This can probably be explained by a low sensitivity of the $d_{z'^2}$−$\pi$(CN) overlap with respect to the Co−NC bending. A similar situation takes place also for the Co(1)−W fragments. The networks of these bonds develop in the plane perpendicular to the plane of the Co(2)−W

bonds (Figure 2S in the Supporting Information), via other cyanide bridges.[1] Because at each W site the $d_{z^2}$ orbital has the same relative orientation with respect to the $\pi$ orbitals of all eight surrounding cyanides, the geometry of the coupling in this network will be obviously the same as that in the previous case. Thus, to a good approximation, the exchange coupling can be considered to be the same for all Co−W pairs in this compound.

Modeling the lowest quintet−triplet splitting by the Heisenberg exchange Hamiltonian $H_{ex} = -J\bar{S}_1\cdot\bar{S}_2$, where $S_1 = {}^3/_2$ is the spin of the Co site and $S_2 = {}^1/_2$ is the spin of the W site, we obtain for $\Delta_{QT} = 11$ cm$^{-1}$ the exchange parameter $J = 5.5$ cm$^{-1}$. From magnetic susceptibility measurements for compound **2**, a value of $\theta = 23.5$ K for the Curie−Weiss constant was derived in the approximation of isotropic exchange coupling.[1] Using the mean-field expression for the Curie−Weiss constant corresponding to two spin sublattices coupled by an isotropic exchange interaction[19]

$$\theta = \frac{J\sqrt{n_1 n_2}}{3k_B}\sqrt{S_1(S_1+1)S_2(S_2+1)}$$

where $n_1 = 4$ and $n_2 = 6$ is the number of nearest-neighboring (exchange-coupled) W ions surrounding a Co ion and vice versa, respectively, we obtain the estimation $J \approx 6$ cm$^{-1}$.

This falls well within the range of values of exchange parameters corresponding to the calculated quintet−triplet gaps in Table 2: $1.5 < J < 10$ cm$^{-1}$.

**Low-Lying Electronic States and the Magnetism of the Co$^{II}$ Fragments.** In order to gain more insight on the mechanism of ferromagnetic coupling in compound **2**, we investigated the effect of the nearest crystal environment on the low-lying electronic states of the mononuclear fragment $[Co(NC)_4(OH_2)_2]^{2-}$. The modeling of the W$^V$ environment by a $Ba^{2+}$ AIMP (as was done in the previous section) yielded a ground state for the Co$^{II}$ complex, which matches well the electronic configuration of the Co ion in the corresponding calculations for the binuclear fragment. That is, the $d_{x^2-y^2}$ orbital of Co now is doubly occupied in the lowest electronic state. Compared to previous calculations for the mononuclear complex (Table 1), the main difference is the crossing of the lowest states $^4B_g{}^1$ and $^4B_g{}^2$, with the last one becoming the ground state. The excitation energy to $^4B_g{}^1$ is 774 cm$^{-1}$, and that to $^4A_g{}^1$ (third row of Table 1) is 963 cm$^{-1}$. The energies of other excitations are modified by less than 1000 cm$^{-1}$ (an exception is the state $^4B_g{}^4$). Thus, the symmetry of the ground state remains unchanged after including the effect of the environment; the same goes for the assignment of ligand-field transitions done in a previous section.

The stabilization of the $d_{x^2-y^2}$ orbital in this calculation can be understood by different effects that the PC or AIMP have on the orbitals from the $t_{2g}$ shell. The stabilization effect of a positive charge on these orbitals comes from two contributions. First, the electrostatic interaction of the electron distributed in these orbitals with the potential of a positive charge always leads to energy lowering. The second, indirect contribution is related to the electrostatic stabilization of $\pi$ and $\pi^*$ orbitals of the cyanide that is in contact with the PC or AIMP. The downshift of these orbitals will enhance the stabilizing effect on the Co $t_{2g}$ orbitals from the covalent interaction with the $\pi^*$ orbitals and will weaken the destabilizing effect from the covalent interaction with the $\pi$ orbitals by modifying the corresponding orbital energy gaps (the diagram in Figure 5). The overall stabilization effect of PC/AIMP on the $t_{2g}$ orbitals of Co can be inferred also from a comparison of the energies of the corresponding active orbitals obtained with and without PC/AIMP (Table 1S in the Supporting Information). Both the electrostatic and the covalent contributions to the stabilization obviously increase with the extent of mixing of the cyanide orbitals into the $t_{2g}$ orbitals of Co. Figure 5 shows the shape of the active orbitals of the $t_{2g}$ type of Co obtained for the experimental geometry of the fragment and optimized positions of the H atoms in the two water molecules. We can clearly observe a greater covalent character of the $d_{x^2-y^2}$ orbital, which implies a stronger stabilization of this orbital by the positive PC or AIMP. One should note, however, that in our modeling of the environment we have neglected the effects of strong covalent bonding between cyanide and W. To understand the stabilizing effect of the W−CN covalence on the $t_{2g}$ orbitals of Co$^{II}$, we should first examine the relative energies of the d orbitals of W and Co. The analysis of energies of active orbitals obtained from CASSCF calculations of the Co−W binuclear fragment in Table 1S in the Supporting Information shows that the $t_{2g}$ orbitals of Co lie lower in energy than the $d_{z^2}$ orbital of W and the other W orbitals of the d type, which are much higher in energy.[20] This means that the $t_{2g}$ orbitals of Co will be stabilized by the covalent

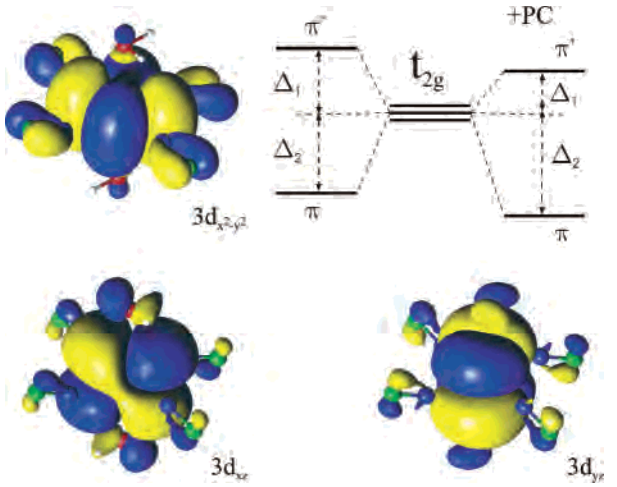


**Figure 5.** Three $d_\pi$ active orbitals ($t_{2g}$ components) of the mononuclear Co fragment. The diagram shows the position of $\pi$ orbitals of cyanide relative to the $t_{2g}$ orbitals of Co.

(19) For example, see: (a) Palacio, F. In *Introduction to Physical Techniques in Molecular Magnetism: Structural and Macroscopic Techniques*; Palacio, F., Ressouche, E., Schweizer, J., Eds.; Servicio de Publicaciones de la Universidad de Zaragoza: Zaragoza, Spain, 1999. (b) Ashcroft, N. W.; Mermin, N. D. *Solid State Physics*; Saunders College: Philadelphia, 1988; Chapter 33.

(20) Hendrickx, M. F. A.; Mironov, V. S.; Chibotaru, L. F.; Ceulemans, A. *Inorg. Chem.* **2004**, *43*, 3142.

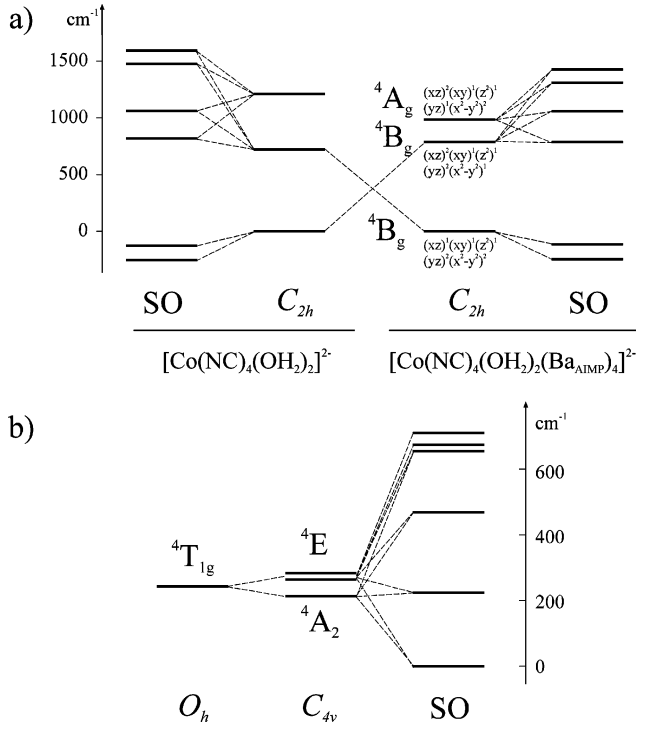


**Figure 6.** Lowest molecular terms and Kramers doublets obtained after including the spin−orbit (SO) interaction for the mononuclear Co fragment in **1**, calculated with and without AIMP by the CASSCF/CASPT2 method in the present work (a) and within the ligand-field model of ref 1 (b).

interaction with the d orbitals of W via cyanide bridges. Given the more pronounced covalent mixing of the cyanide orbitals into the $d_{x^2-y^2}$ orbital of Co as compared to the other two $t_{2g}$ orbitals (Figure 5), this stabilization will again be stronger for this orbital.

To have an additional check for the obtained scheme of lowest energy levels of the Co fragment, it is interesting to simulate its magnetic properties and to compare them with the available magnetic data for compound **1**. To this end, one should take into account the effect of spin−orbit coupling on the lowest states. This was done by allowing spin−orbit mixing of 10 spin quartets and 9 lowest spin doublets of the Co fragment using the RASSI program of *MOLCAS*.[12] The calculated spectrum of lowest Kramers doublets is shown in Figure 6a for an isolated Co fragment and for the case when the $Ba^{2+}$ AIMP was included at the positions of four nearest-neighboring W ions. As we can see, the zero-field splitting of the ground state (117 $cm^{-1}$ for the case when AIMP was included) is much smaller than the energy separation to the Kramers doublets arising from the excited terms $^4B_g{}^1$ and $^4A_g{}^1$. Next the obtained spectrum of spin−orbit states (29 Kramers doublets) was used for the calculation of the Van Vleck susceptibility for powder as a function of the temperature, $\chi(T)$.[13] A comparison with the experimental curve[1] shows that the calculated function $\chi(T)\cdot T$ is situated higher (Figure 3S in the Supporting Information). For instance, at room temperature, the calculated value is 2.985 $cm^3\ mol^{-1}$ K against the experimental value of 2.72 $cm^3\ mol^{-1}$ K. Also, the slopes of the curves differ, with the theoretical one being steeper at low temperatures. The last is due to a smaller gap to the first excited Kramers doublet obtained in our ab initio calculations (Figure 6). Using the same ab initio methodology,[13] we calculated the $g$ tensor for the ground Kramers doublet, which, for the calculation including AIMP, has the main values $g_1 = 2.13$, $g_2 = 3.65$, and $g_3 = 6.31$, corresponding to the magnetic axes $x$, $z$, and $y$, respectively ($y$ coincides with the twofold symmetry axis of the fragment). Note that this $g$ tensor corresponds to an effective spin $\tilde{S} = {}^1/_2$ of the Kramers doublet. The averaging of this tensor gives the $g$ factor 4.38. With the calculated $g$ tensor, we simulated the field dependence of magnetization at $T = 2$ K. Compared to the experimental dependence $M(H)$,[1] the calculated magnetization is higher (Figure 4S in the Supporting Information). One factor that will diminish the calculated $\chi(T)\cdot T$ at low temperatures and $M(H)$ is the antiferromagnetic exchange interaction between $Co^{II}$ fragments. However, this effect is expected to be quite weak in compound **1**. Therefore, the reason for the discrepancies between calculated and measured magnetic properties is that the spectrum of Kramers doublets is not reproduced with enough accuracy by our ab initio calculation, first of all, because of the simplified simulation of the environment with AIMP. Indeed, additional calculations have shown that the obtained solutions are quite sensitive to the way in which we simulate the environment.

The magnetic data of compound **1** have been fitted by Herrera et al.[1] within a ligand-field model approximating the ligand environment of the Co ions by a tetragonally distorted octahedron. The corresponding spectrum of Kramers doublets is calculated in Figure 6b. One can see that without including the spin−orbit coupling the ground octahedral term $^4T_{1g}$ splits into a ground nondegenerate term and an excited twofold degenerate term. The last degeneracy is not supported by symmetry for any conformations of water molecules and cyanide groups. The energy separation between the terms is also rather small (100 $cm^{-1}$).[1] As our calculations show, such a spectrum of lowest molecular terms cannot be obtained for an isolated $[Co(NC)_4(OH_2)_2]^{2-}$ complex whatever the conformation is (Figures 2 and 6b). Therefore, if such an ordering of the lowest levels really exists, it is essentially determined by the interaction of the fragment with the environment. Indeed, as Figure 6a shows, including the AIMP in the calculation brings the picture of three molecular levels closer to the fitted one. Moreover, the nature and the symmetry of the ground term is the same as those in the ligand-field model in Figure 6b. This resolves the uncertainty about the order of the lowest terms in ref 1. However, the spectra of Kramers doublets predicted by the two approaches differ drastically. In the fitted ligand-field model, the splitting of the $^4T_{1g}$ term was obtained much smaller than the spin−orbit coupling constant for the $Co^{2+}$ ion ($\zeta = 530$ $cm^{-1}$). This means that the orbital momentum on the Co ion is predicted to be almost unquenched; i.e., in the first approximation, the spin−orbit multiplets are eigenfunctions of the total momentum $J$, which is the sum of the spin momentum $S = {}^3/_2$ and the effective orbital momentum corresponding to the $t_{2g}$ shell, $L = 1$.[21] The resulting three

(21) Griffith, J. S. *The Theory of Transition-Metal Ions*; University Press: Cambridge, U.K., 1971.

spin−orbit multiplets with $J = {}^5/_2$, ${}^3/_2$, and ${}^1/_2$ will split in the tetragonal ligand field into degenerate pairs of states corresponding to $\pm M_J$, which gives the six Kramers doublets in Figure 6a. The ground state corresponds almost completely to the multiplet with $J = {}^1/_2$ (the admixture coefficient is 0.99), which means that the corresponding Kramers doublet is almost isotropic. By contrast, the ground Kramers doublet was obtained in our ab initio calculations strongly anisotropic because it arose from the zero-field splitting of the ground-state spin $S = {}^3/_2$. Moreover, the main anisotropy axis in our calculation is the twofold rotational axis *y* and not the axis passing through the water ligands (*z* in Figure 1) as supposed by the ligand-field model. The fitted value of the *g* factor for the lowest Kramers doublet in the ligand-field model is $g = 4.04$, i.e., lower than the one we have obtained by averaging the *g* tensor (4.38), which explains why our ab initio simulations give higher values for susceptibility and magnetization. Despite the fact that the agreement between the ab initio simulations and the ligand-field modeling concerning the spectrum of Kramers doublets is not perfect,[22] there are no doubts that the ground term corresponds to the configuration $(yz)^2(x^2 - y^2)^2(xz)^1(z^2)^1(xy)^1$, as is obtained in both approaches.

Thus, the ground electronic state of the Co fragment in compound **1** supports the electronic configuration on the Co sites found for the lowest states of the binuclear Co−W fragments of compound **2**. This is important because we were able to perform more accurate calculations for the mononuclear Co fragment, by taking into account the double-shell effect in CASSCF calculations. The reason for the observed ferromagnetic coupling in these fragments seems definitely to be the double occupation of the $d_{x^2-y^2}$ orbital on Co and the consequent quenching of the electron delocalization between magnetic orbitals via the bridging cyanide. One should mention that an alternative mechanism of ferromagnetic interaction in binuclear metal fragments involving $d^1$ octacyanometallates was earlier proposed,[15] stressing the importance of the contribution arising from the delocalization of magnetic electrons into unoccupied orbitals of another metal site.[23] This contribution arises from a joint effect of strong electron delocalization via the $\sigma$ orbitals of cyanide into the empty orbitals of octacyanometallate and the Hund interaction of the transferred electron with the unpaired electron in the lowest orbital on the octacyano metal site. The estimations in ref 15 have shown that this ferromagnetic contribution can overcome the antiferromagnetic kinetic contribution arising from the delocalization of magnetic electrons via the $\pi$ orbitals of the cyanide bridges provided the Hund rule coupling parameter *I* is not smaller than 0.5 eV. Although this value is well within the expectations for transition-metal complexes,[21] the estimation of Racah parameters from CASSCF/CASPT2 calculations for tungsten(IV) and molybdenum(IV) octacyano complexes gave values much lower than expected.[20] In the case of $[W(CN)_8]^{4-}$, these are $B = 100$ cm$^{-1}$ and $C = 400$ cm$^{-1}$, giving for the Hund rule coupling $I = C + 3B = 700$ cm$^{-1}$, a value several times smaller than expected, at the same rate reducing the expected ferromagnetic kinetic contribution.[24] Moreover, there is also a small mixing of the $d_{z'^2}$ orbital of W with the $d_{z^2}$ orbital of Co via the $\sigma$ orbitals of cyanide, which opens an additional channel of antiferromagnetic interaction via spin delocalization through $\sigma$ orbitals. One should mention that the antiferromagnetic interaction in cyano-bridged bimetallic fragments involving $d^1$ octacyanometallates was also obtained in density functional theory calculations of the cyano-bridged complex $Mo_6Mn_9$, where the delocalization of the magnetic electron on each $Mo^V$ center to neigboring Mn sites via the $\pi$ orbitals of the cyanide bridges is present.[25]

## Conclusions

We have investigated the origin of ferromagnetic interaction in the three-dimensional magnetic network $[\{W^V(CN)_2\}_2\{(\mu\text{-}CN)_4Co^{II}(H_2O)_2\}_3\cdot 4H_2O]$ (**2**) by CASSCF/CASPT2 calculations of mononuclear Co and binuclear Co−W fragments.

We studied different structural models of isolated fragments, including the effect of the environment, by these ab initio methods and calculated the exchange interaction parameter, the energies of the ligand-field transitions, and the magnetic properties of the mononuclear Co fragment (the temperature-dependent magnetic susceptibility, the *g* tensor, and the field-dependent magnetization). These results have been compared with available data for compounds **1** and **2** and with the predictions of the ligand-field model used for the fitting of the magnetic data of compound **1** in ref 1. In agreement with the suggestion made in ref 1, we have found that in both magnetic networks the ground state of the Co fragment is characterized by the electronic configuration where the single $d_\pi$ orbital on the Co site ($d_{x^2-y^2}$), which can covalently mix with the magnetic orbital on the W site ($d_{z'^2}$), is doubly occupied. This condition is crucial for the existence of ferromagnetic interaction between Co and W sites in **2**. We have shown that the above electronic configuration on the Co sites cannot be achieved in mono- and binuclear metal fragments in **1** and **2** unless the interaction of the Co fragment with the environmental atoms is taken into account. This result shows that the tuning of orbitals responsible for magnetism is a more involved phenomenon than was thought before and the role of distant coordination spheres can become crucial in some complexes containing open-shell electronic configurations with closely spaced orbitals. The effect reported here becomes more pronounced when the interaction of the chosen fragment with the neighboring coordination sphere of metal ions is relatively strong. It is expected to be particularly important for the cases when the

(22) One should have in mind that the ligand-field model is also quite approximate, especially with regards to the simulation of low-symmetry structural effects.

(23) Goodenough, J. B. *Magnetism and Chemical Bond*; Interscience: New York, 1963; Chapter 5.

(24) The obtained low values of the Racah parameters and of the Hund rule coupling are due to the strong covalent admixure of cyanide orbitals to the metal d orbitals in cyano complexes involving metals from the second and third transition row.

(25) Ruiz, E.; Rajaraman, G.; Alvarez, S.; Gillon, B.; Stride, J.; Clerac, R.; Larionova, J.; Decurtins, S. *Angew. Chem., Int. Ed.* **2005**, *44*, 2711.

metals interact with each other directly by through-space interaction[26,27] or form metallic bonds.[28,29]

**Acknowledgment.** Financial support by the Belgian Science Foundation and Flemish Government under the Concerted Action Scheme is gratefully acknowledged. A.S. is thankful for financial support from the Francqui Foundation. We thank Prof. Michel Verdaguer for useful discussions.

(26) Glaser, T.; Beissel, T.; Bill, E.; Weyhermüller, T.; Schünemann, V.; Meyer-Klaucke, W.; Trautwein, A. X.; Wieghardt, K. *J. Am. Chem. Soc.* **1999**, *121*, 2193. Chibotaru, L. F.; Girerd, J.-J.; Blondin, G.; Glaser, T.; Wieghardt, K. *J. Am. Chem. Soc.* **2003**, *125*, 12615.

(27) Ceulemans, A.; Chibotaru, L. F.; Heylen, G. A.; Pierloot, K.; Vanquickenborne, L. G. *Chem. Rev.* **2000**, *100*, 787.

(28) Cotton, F. A.; Walton, R. A. *Multiple Bonds between Metal Atoms*; Oxford University Press: Oxford, U.K., 1993.

(29) Clérac, R.; Cotton, F. A.; Daniels, L. M.; Dunbar, K. R.; Kirschbaum, K.; Murillo, C. A.; Pinkerton, A. A.; Schultz, A. J.; Wang, X. *J. Am. Chem. Soc.* **2000**, *122*, 6226.

**Supporting Information Available:** Information on the active orbitals for the binuclear Co−W fragment (Table 1S), plots of four antibonding active orbitals (Figure 1S), arrangement of the W sites around the Co1 fragment in **2** (Figure 2S), and ab initio simulations of the magnetic properties of the Co fragment in **1** (Figures 3S and 4S). This material is available free of charge via the Internet at http://pubs.acs.org.

IC062345+